Effect of a single water molecule on the conformational preferences of a capped Pro–Gly dipeptide in the gas phase

Sourav Mandal, Arsene Kossov, Pierre Carcabal, Aloke Das

Effect of a single water molecule on the conformational preferences of a capped Pro-Gly dipeptide in the gas phase

Sourav Mandal,[1,#] Arsene Kossov,[2,#] and Pierre Carcabal,[2,a)] Aloke Das[1,a)]

[1]Department of Chemistry, Indian Institute of Science Education and Research Pune, Dr. Homi Bhabha Road, Pashan, Pune 411008, India

[2]Institute des Sciences Moleculaires d'Orsay, Universite Paris-Saclay, CNRS, 91405 Orsay, France

[a)]Authors to whom correspondence should be addressed: a.das@iiserpune.ac.in, pierre.carcabal@cnrs.fr

[#]Equal contribution

ABSTRACT

Herein, we have investigated the effect of microhydration on the secondary structure of a capped dipeptide Boc-^{D}Pro-Gly-NHBn-OMe (Boc= tert-butyloxycarbonyl, Bn = Benzyl), i.e., PG with a single H_2O molecule using gas-phase laser spectroscopy combined with quantum chemistry calculations. Observation of a single conformer of the monohydrated peptide has been confirmed from IR-UV hole-burning spectroscopy. Both gas-phase experimental and theoretical IR spectroscopy results confirm that the H_2O molecule is inserted selectively into the relatively weak C7 hydrogen bond (γ-turn) between the Pro C=O and NHBn N-H groups of the peptide, while the other C7 hydrogen bond (γ-turn) between the Gly N-H and Boc C=O groups remains unaffected. Hence, the single H_2O molecule in the PG$\cdots(H_2O)_1$ complex significantly distorts the peptide backbone without appreciable modification of the overall secondary structural motif (γ-γ) of the isolated PG monomer. The nature and strength of the intra- and inter-molecular hydrogen bonds present in the assigned conformer of the PG$\cdots(H_2O)_1$ complex has also been examined by natural bond orbital (NBO) and non-covalent interaction (NCI) analyses. The present investigation on the monohydrated peptide demonstrates that several H_2O molecules may be required for switching the secondary structure of PG from the double γ-turn to a β-turn that is favorable in the condensed phase.

I. INTRODUCTION

Secondary structures of peptides contribute significantly to the specific three-dimensional structures of proteins.[1-3] The three most common secondary structures of peptides are α-helix, β-sheet, and turns, which are formed due to intramolecular hydrogen bonding interactions between the NH and C=O groups of the backbone of peptides.[4-7] Turns are of different types, such as, α, β, and γ depending on 13 (C13), 10 (C10), and 7 (C7) membered hydrogen-bonded ring formation at the backbone involving $i \rightarrow i + 4$, $i \rightarrow i + 3$, and $i \rightarrow i + 2$ residues, respectively, as shown in scheme 1.[8-10] A particular turn structure at a required location of the peptide backbone also depends on the presence of specific amino acid residues and their sequence. Gly and Pro being the most flexible and rigid amino acid residues, respectively, are abundant in the loop regions of the β-hairpin structures of proteins.[11, 12] Nevertheless, the Pro-Gly sequence is more prominent than the Gly-Pro in terms of the β-turn formation, which is a mandatory requirement for the loop.[13-15] On the contrary, the Gly-Pro sequence is more prone to forming an extended polyproline (PP)-II structure.[13, 15]

The secondary structures of the peptides, governed by local interactions, can be studied at the smaller peptide levels i.e., dipeptides, tripeptides, etc., by protecting both the -N and -C terminals, which can mimic further higher-order peptides.[16] Gas phase laser spectroscopic studies can explore the intrinsic structures of several low-energy conformations of isolated peptides.[17-32] Alternatively, in the solution phase studies, one can obtain information on either the most stable conformation or an average structure over several conformations. On the other hand, the study of microhydrated peptides can reveal the influence of a limited and controlled number of water molecules on the conformational preferences of model peptidic sequences, in comparison to the intrinsic preferences of the same models fully isolated in the gas phase, free of any environmental perturbation. These data can bridge the spectroscopic results or information obtained from the isolated gas phase and solution phase studies of the peptides,

and render evidence of the potential role of structural water molecules in direct, specific, and local interactions with peptides and specifically affecting their structure, and hence their functioning, in a bulk aqueous environment.

There are numerous reports on gas-phase studies of microsolvation of small molecules, starting from rigid systems such as benzene or phenol to flexible ones like neurotransmitters, amino acids (capped and uncapped), sugars, etc.[33-43] However, similar gas phase microhydration studies on peptides are scarce in the literature, although a significant number of reports exploring the spectral signatures of low-energy conformers of isolated small peptides are present there. It has been demonstrated from gas-phase spectroscopy that five CH_3OH molecules are required to obtain the zwitterionic solution-phase structure of an amino acid tryptophan from its gas-phase neutral structure.[38] In the case of a capped phenylalanine (CH_3CO-Phe-NH_2), it has been found that a single water molecule can induce the folding of a β-strand into a γ-turn structure in the gas phase.[41]

Despite the potential of the microsolvated gas-phase spectroscopy to reveal the structures of both unprotected and protected amino acids with a controlled number of solvent molecules, microsolvation studies of only three peptides i.e., Ac-Val-Tyr(Me)-NHMe$\cdots(H_2O)_1$, Z-Aib-Pro-NHMe$\cdots(CH_3OH)_{1\text{-}2}$ [Z = benzyloxycarbonyl], and cyclo[L-Tyr(Me)-D-Pro]$_2\cdots(H_2O)_1$ are so far reported in the literature.[44-46] Of course, the scanty nature of the microsolvated gas phase studies of the peptides in the literature is due to the challenging task of achieving sufficient cooling in the jet expansion in the presence of laser desorption to vaporize peptides. The most intriguing observation from these meager microsolvated studies of the peptides is the complexation of the capped dipeptide Z-Aib-Pro-NHMe with the sequential addition of CH_3OH molecules. The isolated dipeptide, as well as its complex with one CH_3OH, i.e., Z-Aib-Pro-NHMe$\cdots(CH_3OH)_1$, opts for a γ-turn structure, while the addition of only two CH_3OH

molecules can switch the γ to the β-turn conformation of the peptide in the gas phase, which is the preferred structure in the condensed phase.[45]

In this work, we have investigated the effect of a single H_2O molecule on the conformational preference of a capped dipeptide Boc-^{D}Pro-Gly-NHBn-OMe (PG) in the gas phase using resonant 2-photon ionization (R2PI) and IR-UV double resonance spectroscopy combined with quantum chemistry calculations. It has been reported that the PG peptide in the gas phase exhibits a double γ-turn conformation, while the preferred conformation of the peptide in the solution phase is the β-turn.[21] The present work aims to determine whether the first H_2O molecule can change the isolated gas phase secondary structure of PG to a structure similar to the solution phase or simply distort the peptide's backbone without significantly modifying the secondary structure.

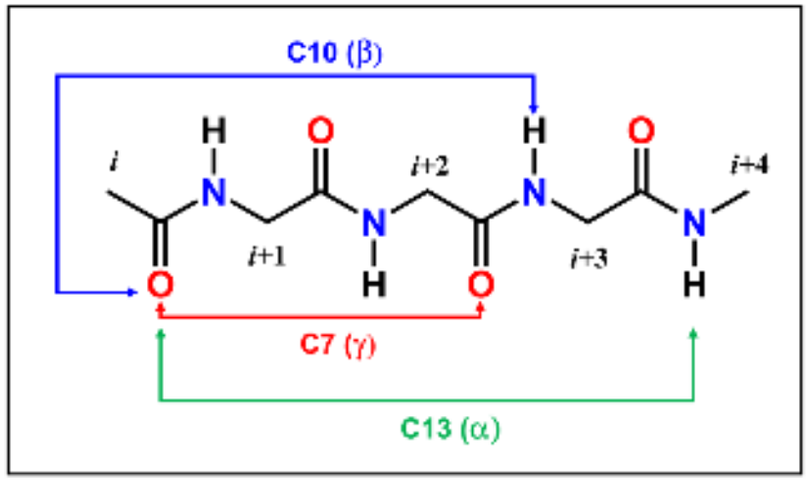

Scheme 1. A schematic diagram showing different types of turns in a polypeptide backbone. *i, i+1, i+2, i+3, and i+4* represent the peptide residue numbers.

II. METHODS

A. Experimental

The peptide PG was synthesized by following a procedure that is known in the literature[47] and also described in the spectroscopic studies of the PG monomer reported earlier.[21] The

experimental results reported in this work rely on mass-resolved, conformer-selective IR-UV double resonance spectroscopy of supersonically cooled laser-desorbed non-volatile species, as already described elsewhere.[43] The experimental approach is well-established and has been extensively used to obtain conformer-selective and mass-resolved vibrational spectra of non-volatile compounds and clusters in the gas phase, including biomolecules[32,48]

Briefly, it consists of a time-of-flight mass spectrometer (Jordan TOF Products, Inc.) coupled to a pulsed supersonic expansion seeded by the molecules under study, that are vaporized upon laser desorption. The laser desorption samples were prepared by dissolving PG in ethanol at a concentration of 5 mg/mL and spraying this solution with an aerograph on the surface of a solid graphite bar to create a thin uniform layer of the molecules of interest, using the method described before.[43] The graphite bar was subsequently placed inside the vacuum chamber next to the nozzle of a 500 μm pulsed supersonic valve (Jordan PSV, 10 Hz, 5 bars of Neon). The deposited molecules were desorbed by focusing the Nd:YAG laser (1064 nm, Minilite Continuum, 10Hz, 500 μJ/pulse) onto the surface of the sample. The evaporated molecules were coupled to the supersonic expansion, where they were cooled down, and the hydrated complexes were stabilized by the collisions with the buffer gas. To produce the hydrated complexes, room temperature vapor pressure of water (either H_2O or D_2O) was seeded with the carrier gas upstream of the jet nozzle. Since the laser desorption sample is located in the vacuum, the molecules under study are not exposed to the water isotopomers before they are evaporated and incorporated inside the supersonic expansion, downstream of the jet. This prevents H/D exchange between heavy water and the desorbed molecules, and avoids distributing the isotopes over all labile protons of the system.[43]

The molecules and complexes of interest were entrained towards the ionization region of a linear TOF mass spectrometer through a 3 mm skimmer in the differentially pumped detection chamber, where they interacted with the UV and IR lasers. The electronic spectra of the

complexes were observed by applying a 2-color Resonantly Enhanced Multiphoton Ionization 2c-REMPI 1+1' scheme (2c-R2PI). A first tunable UV laser (355 nm pumped dye laser, PDL3000, Lambda Physics, Coumarin 540A, 500 μJ/pulse, 265-285 nm, frequency double with a BBO crystal) was used to excite the S_0-S_1 vibronic transitions, and ionization from the S_1 state was achieved by a second ionization laser (532 nm pumped OPO, Continuum Horizon, 330 nm, 20 mJ/pulse). To perform resonant ion-dip infrared spectroscopy (RIDIRS) or IR-UV hole-burning spectroscopy[32], IR radiation was obtained from the idler of a tunable OPO/OPA system (LaserVision, 5 mJ/pulse, 2.5 – 4 μm). In the case of the RIDIRS, the IR laser is scanned in the desired wavelength region by keeping the UV laser wavelength fixed, while the opposite scheme is used for the IR-UV hole-burning spectroscopy, i.e., the UV laser is scanned while fixing the IR laser wavelength.

B. Computational

Structures of the observed conformer of PG···$(H_2O)_1$ are determined through exhaustive conformational sampling using the Molclus program[49] based on molecular dynamics, followed by quantum chemistry calculations employing the Gaussian 09 suite of programs.[50] It has been reported in the literature that the distribution of the monohydrated conformations of the peptides is governed by the distribution of the initial monomer conformations.[41] The experimentally observed conformers of the PG monomer in the gas phase reported earlier are PG-C7$_D$-C7$_L$-g^+-c and PG-C7$_D$-C7$_L$-g^+-t.[21] Figure 1a depicts a chemical structure of PG representing the C7$_D$-C7$_L$ backbone of the two conformers, while the ball and stick structure of the most stable conformer of the PG monomer optimized at the M06-2X/6-311++G(d,p) level of theory is presented in Figure 1c. Atom numbering and labeling of the Ramachandran angles (ϕ_1, ψ_1, ϕ_2, and ψ_2), including other relevant dihedral angles defining the conformational landscape of the PG monomer, are also provided in Figure 1a. Both the observed conformers

of PG have $C7_D$-$C7_L$ backbone where the first C7 hydrogen bond is between the C=O group of Boc and N-H group of Gly while the C=O group of Pro and benzyl (Bn) N-H form the 2nd C7 hydrogen bond. Here, $C7_D$ is due to $+\phi_1$, $-\psi_1$ backbone orientation while the opposite one, i.e., $-\phi_1$, $+\psi_1$ orientation, is termed $C7_L$.[17] The χ_2 dihedral angles of +60°, -60°, and 180° due to the rotation of the benzyl group along the N_{20}-C_{22} bond generate g^+, g^- (*gauche*), and *a* (*anti*) conformers, respectively. *c* and *t* notations denote the *cis* and *trans* orientations of the OMe group of the benzyl moiety with the χ_4 dihedral angles of 0° and 180°, respectively. The χ_3 and χ_1 dihedral angles denote the rotation of the phenyl and OBu^t groups along the C_{22}-C_{23} and O_5-C_6 bonds, respectively. Figure 1b shows a chemical structure of another class of a probable low-energy conformer of the PG monomer with C10 backbone, i.e., PG-F-C10-g^--*c*, which was not observed in the gas phase.[21] The C10 hydrogen bond in PG-F-C10 is present between the C=O group of Boc and benzyl (Bn) N-H group while the Gly N-H is free, and hence, it is denoted as F.

First, we generated about 1000 conformers of PG···$(H_2O)_1$ each with the PG-$C7_D$-$C7_L$-g^+-*c*, PG-$C7_D$-$C7_L$-g^+-*t*, and PG-F-C10-g^--*c* conformers of the peptide monomer using the Molclus program. A total of 3000 conformers of PG···$(H_2O)_1$ were optimized initially at the HF/6-31G(d) level. Afterward, all the conformers, optimized at the HF/6-31G(d) level, were grouped based on the similarity in the energies within the 0.1 kJ/mol window as well as their structures, and vibrational frequencies. This clustering process reduced the number of conformers to 200, which were further optimized at the M05-2X/6-31+G(d) level. Then, the M05-2X level optimized structures were checked for redundancy, i.e., structural similarity and energies within the 0.3 kJ/mol window. Finally, 37 conformers with an energy cut-off of 20 kJ/mol were optimized at the M06-2X/6-311++G(d,p) and B3LYP-D3/def2-TZVPP levels of theory followed by their vibrational frequency calculations at the same levels. The lack of any imaginary frequency ensured that all the optimized structures were energy minima only. Final

optimized structures were checked for any redundancy. Energies of the conformers were corrected for zero-point energies (ZPE), basis set superposition error (BSSE)[51], and thermal energies. Special attention was also provided to verify that Molclus could generate conformers encompassing the binding of H_2O to all probable hydrogen bonding sites of PG. Furthermore, the energies of a few conformers (up to 8 kJ/mol) optimized at the M06-2X/6-311++G(d,p) and B3LYP-D3/def2-TZVPP levels were refined by single point (SP) energy calculation at the MP2 level. Intra- and inter-molecular hydrogen bonding interactions present in the observed conformers of PG···$(H_2O)_1$ were examined using natural bond orbital (NBO) and noncovalent interaction (NCI) analyses.[52-55]

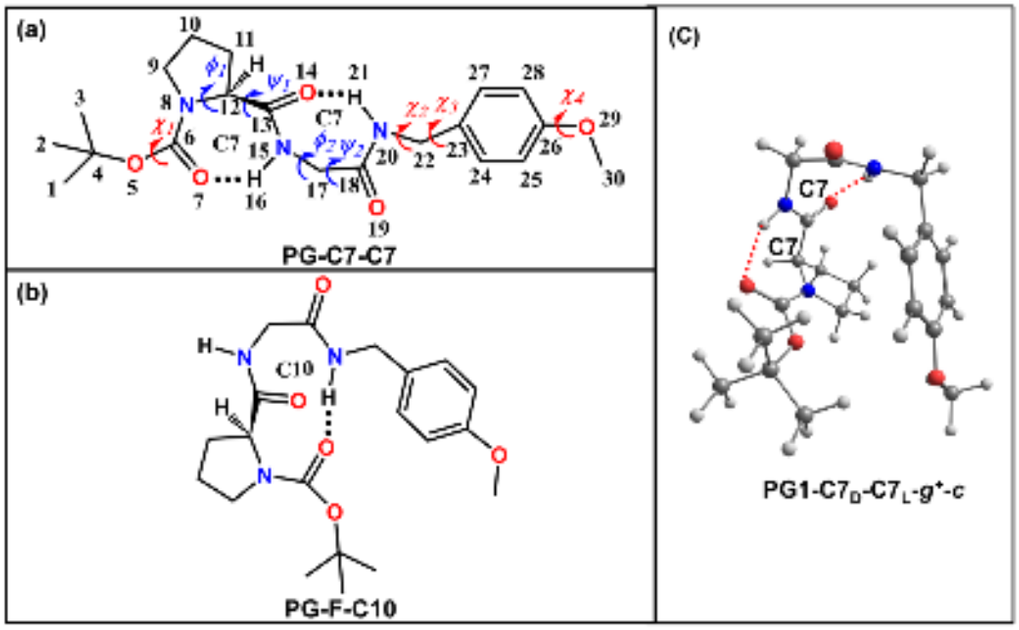

Figure 1. Chemical structures of the PG monomer with (a) $C7_D$-$C7_L$ and (b) F-C10 backbones. Atom numbering and marking of important dihedral angles of the peptide are shown in Figure 1a. (c) Ball and stick structure of the most stable conformer of the PG monomer optimized at the M06-2X/6-311++G(d,p) level of theory.

III. RESULTS AND DISCUSSION

A. Computational conformational landscape of PG···$(H_2O)_1$

Figure 2a displays an energy level diagram of a few low-energy conformers of PG···$(H_2O)_1$ optimized at the M06-2X/6-311++G(d,p) level. ZPE and BSSE corrected relative Gibbs free

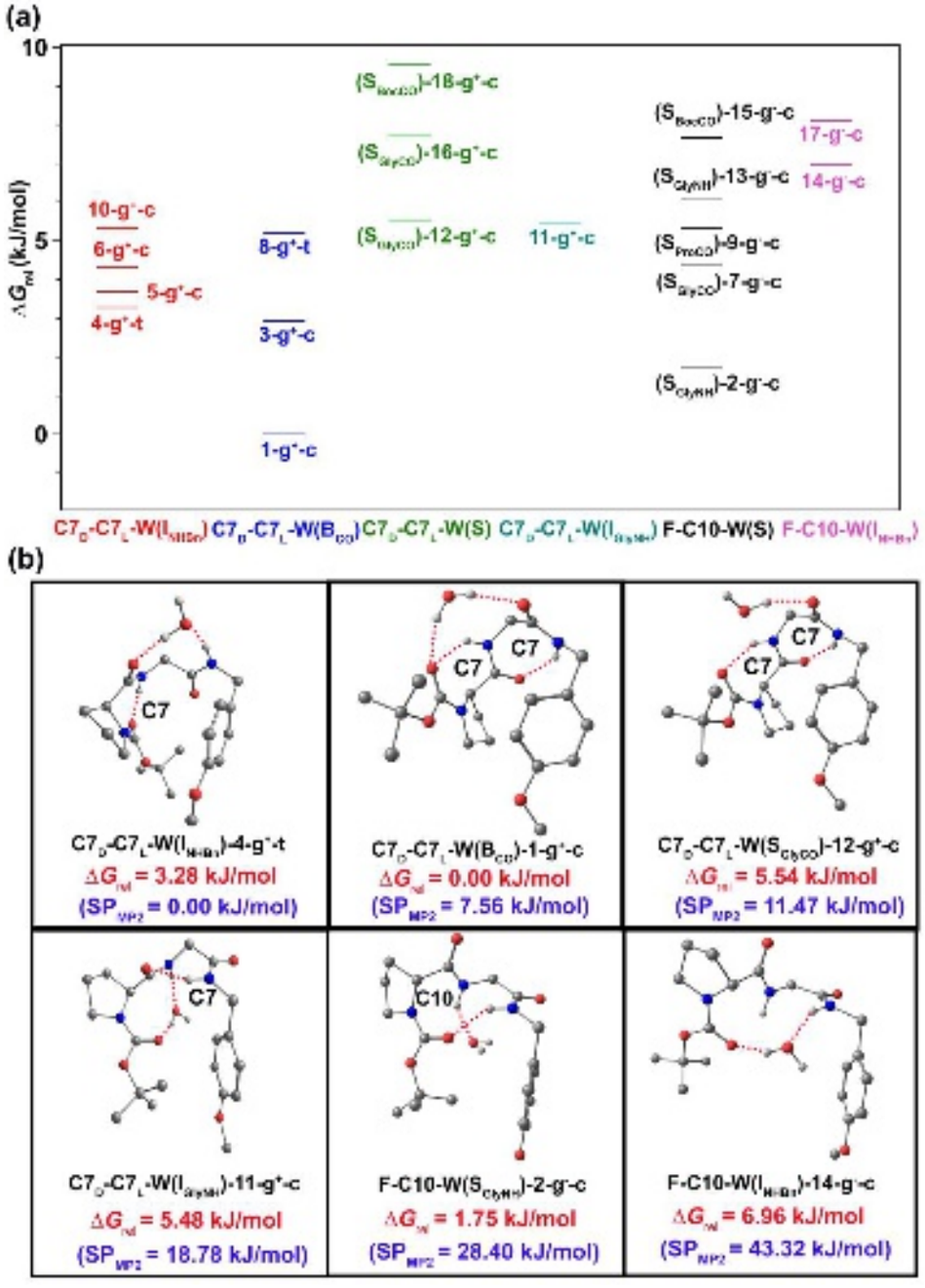

Figure 2. (a) Energy landscape of a few low-energy conformers of the PG···$(H_2O)_1$ complex calculated at the M06-2X/6-311++G(d,p) level of theory. $\Delta \boldsymbol{G}_{rel}$ stands for ZPE and BSSE corrected relative Gibbs free energies of the conformers at 300 K with respect to that of the most stable conformer. The naming of the conformers and classification of them into six categories are described in the text. (b) One representative structure under each of the six categories optimized at the M06-2X/6-311++G(d,p) level of theory. SP_{MP2} denotes the BSSE corrected MP2 single point energy at 0 K calculated at the MP2/6-311++G(d,p)//M06-2X/6-311++G(d,p) level.

energies (ΔG_{rel}) of the conformers up to 10 kJ/mol at 300 K with respect to the Gibbs energy of the global minimum conformer are shown in the figure. The conformers of PG$\cdots$(H$_2$O)$_1$ are classified into six major categories in terms of the binding of H$_2$O as insertion, bridging, and free sites of solvation of the PG-C7-C7 and PG-F-C10 backbone arrangements of the monomer. One representative structure corresponding to each of the six categories optimized at the M06-2X/6-311++G(d,p) level is provided in Figure 2b, while a complete list of all the structures with ΔG_{rel} up to10 kJ/mol is presented in Figure S1. The numbering of the conformers was done in terms of their energetics at the M06-2X/6-311++G(d,p) level, with the global minimum conformer as number 1. The same numbering of the conformers was maintained at other levels of calculations, irrespective of their energetic order at those levels.

The category C7$_D$-C7$_L$-W(I$_{NHBn}$) indicates that the H$_2$O molecule is inserted into the C7 hydrogen bond between the NHBn and Pro C=O groups of the peptide backbone. Insertion of the H$_2$O molecule into the other C7 hydrogen bond between the Gly NH and Boc C=O groups of the peptide backbone is termed C7$_D$-C7$_L$-W(I$_{GlyNH}$). In the case of C7$_D$-C7$_L$-W(B$_{CO}$), the two C7 hydrogen bonds of the peptide backbone remain unaffected, but the H$_2$O molecule bridges the Gly C=O and Boc C=O groups and forms an additional 12-membered hydrogen bonded ring (C12). C7$_D$-C7$_L$-W(S) category is about the solvation of the peptide through binding of the H$_2$O molecule at one of the free sites such as Gly CO and Boc CO, termed further W(S$_{GlyCO}$), and W(S$_{BocCO}$), respectively. In the case of the C10 backbone of PG, the category F-C10-W(I$_{NHBn}$) designates that the H$_2$O molecule is inserted into the C10 hydrogen bond between the NHBn and Boc C=O groups of the peptide backbone. The category F-C10-W(S) specifies that the H$_2$O molecule is solvated at the free sites, including Gly CO, Pro CO, Gly NH, and OBu^t, termed further W(S$_{GlyCO}$), W(S$_{ProCO}$), W(S$_{GlyNH}$), and W(S$_{OBut}$), respectively. It can be noticed from Figure 2 that the M06-2X/6-311++G(d,p) level predicts C7$_D$-C7$_L$-W(B$_{CO}$)-1-g^+-t, i.e., the bridge conformer as the global minimum although the MP2/6-

311++G(d,p)//M06-2X/6-311++G(d,p) single point energy calculation shows that PG-C7$_D$-C7$_L$-W(I$_{NHBn}$)-4-g^+-t, i.e., the insertion structure is the most stable conformer.

B. Electronic spectroscopy of PG···(H$_2$O)$_1$

Mass-selected electronic spectrum of PG···(H$_2$O)$_1$ measured by the 2c-R2PI technique is displayed in Figure 3b. The electronic spectrum of the PG monomer, which was reported earlier in the literature[21], is reproduced in Figure 3a only to have a comparison with its monohydrated spectrum. Two conformers of the PG monomer A and B, with their electronic origin bands for the $S_1 \leftarrow S_0$ excitation at 35416 and 35442 cm^{-1}, respectively, are reported in the literature. The lowest energy transition, i.e., the electronic band origin of the PG···(H$_2$O)$_1$ complex observed at 35330 cm^{-1}, is red-shifted by 86 cm^{-1} with reference to that of the conformer A of the PG monomer.

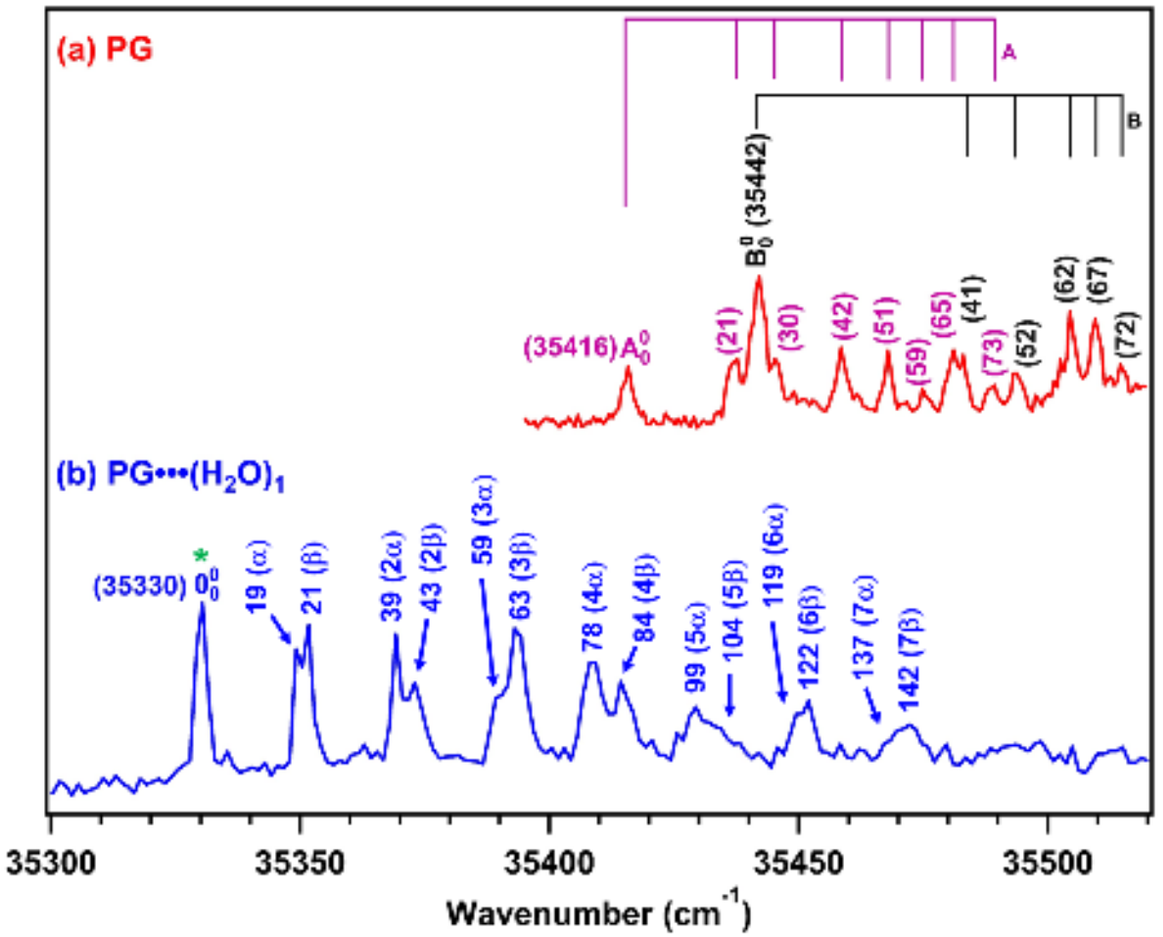

Figure 3. Electronic spectra measured in the mass channels of the (a) PG monomer[21] and (b) PG···$(H_2O)_1$ complex using the 1c-R2PI and 2c-R2PI techniques, respectively. Low-frequency vibrations (in cm^{-1}) of the two conformers (A and B) of PG and a single conformer of the complex are marked with each of the vibronic bands. In the case of PG···$(H_2O)_1$, the low-frequency vibrations are tentatively assigned as progressions of two modes α and β. The presence of a single conformer of the complex is determined from IR-UV hole-burning spectra presented in Figure S2. The electronic origin band, marked with an asterisk in Figure 3b, was probed using RIDIR spectroscopy.

The red shift in the electronic origin band of the complex indicates that the stability of the complex with respect to the monomer in the S_1 state is more than that in the S_0 state. The electronic spectrum of the PG monomer is very much congested with low-frequency intramolecular vibrations due to the libration/torsional motion of the flexible Boc and NH-Bn-OMe groups as well as the intramolecular hydrogen bonds present there (Figure 3a). These low-frequency intramolecular vibrations are also present in the electronic spectrum of the PG···$(H_2O)_1$ complex. However, additional intermolecular vibrations in the complex due to hydrogen bonding between PG and H_2O appear at frequencies similar to some of the intramolecular vibrations present in the PG monomer, and there is a coupling between these intra and intermolecular vibrations. Hence, it is not straightforward to assign the bands in the electronic spectrum (Figure 3b) of the complex arising from the intermolecular vibrations involving H_2O. Nevertheless, observation of a single conformer of the complex is determined from IR-UV hole-burning spectra presented in Figure S2. Thus, the vibronic bands observed in the electronic spectrum of PG···$(H_2O)_1$ are tentatively assigned as the Franck-Condon progressions of two low-frequency modes α (19 cm^{-1}) and β (21 cm^{-1}) of the conformer.

C. IR spectroscopy of PG···$(H_2O)_1$ complex

Figure 4a presents the IR spectrum of PG···$(H_2O)_1$ measured in the N-H and O-H stretching regions by probing its electronic origin band (35330 cm^{-1}), marked with an asterisk in Figure 3b, employing RIDIR spectroscopy. Theoretical scaled IR spectra of a few low-energy conformers of PG···$(H_2O)_1$, with ΔG_{rel} up to 4 kJ/mol, calculated at the M06-2X/6-311++G(d,p) level are provided in Figure 4b-f as stick diagrams. The calculated harmonic NH frequencies of different conformers of PG···$(H_2O)_1$ were corrected using a scaling factor of 0.949 derived from the ratio of the experimental N-H stretching frequency of Z-Gly-OH reported in the literature[26] to the corresponding harmonic N-H frequency of Z-Gly-OH obtained from the M06-2X/6-311++G(d,p) level of calculation. The calculated OH frequencies of PG···$(H_2O)_1$ were scaled using a factor of 0.939 obtained from the ratio of the experimental

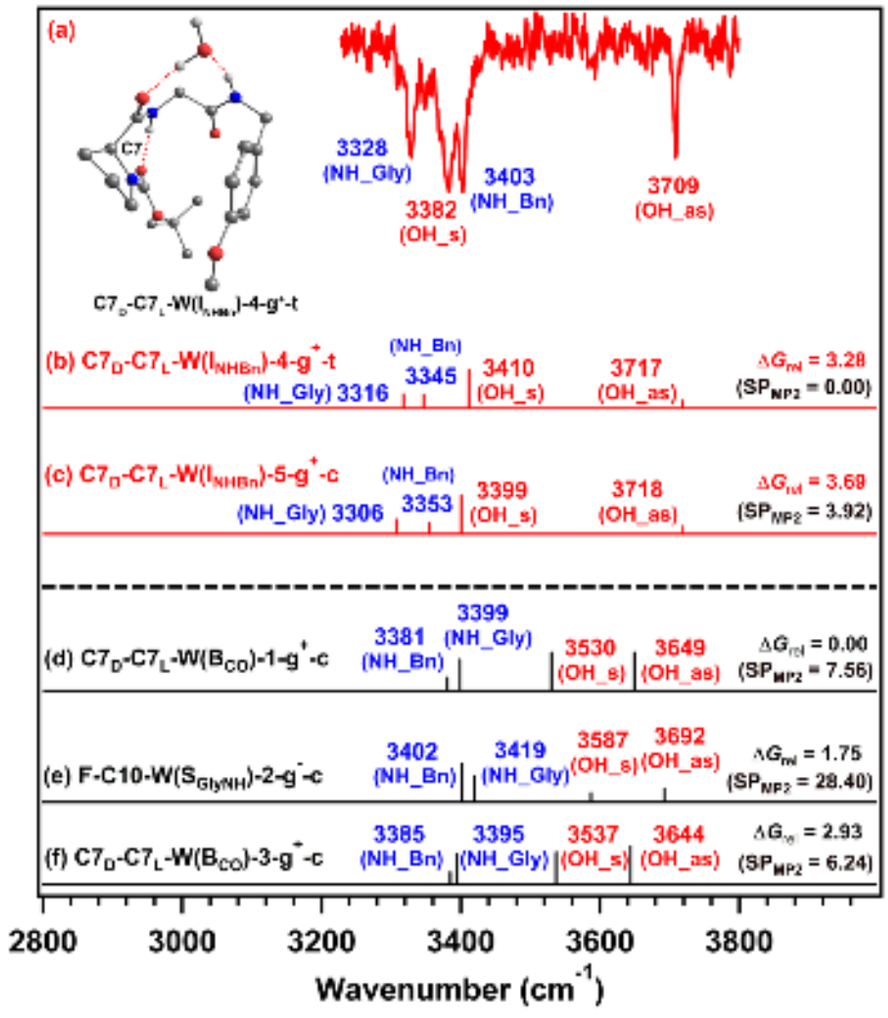

Figure 4. (a) IR spectrum of the PG···$(H_2O)_1$ complex in the N-H and O-H stretching regions measured by RIDIR spectroscopy. (b-f) Theoretical scaled IR stick spectra of a few low-energy conformers of PG···$(H_2O)_1$ up to $\Delta \boldsymbol{G}_{rel}$ = 4 kJ/mol, calculated at the M06-2X/6-311++G(d,p) level of theory. MP2 single point energies (SP_{MP2}) of the conformers calculated at the MP2/6-311++G(d,p)//M06-2X/6-311++G(d,p) level are also provided with the stick spectra. The theoretical harmonic N-H and O-H stretching frequencies of all the conformers are scaled with scaling factors of 0.949 and 0.939, respectively (see the text). The assigned structure of PG···$(H_2O)_1$ is provided with the experimental IR spectrum. OH_as and OH_s denote antisymmetric and symmetric stretching vibrations of H_2O, respectively.

antisymmetric OH stretching frequency of free H_2O in the gas phase to the corresponding OH frequency of H_2O calculated at the M06-2X/6-311++G(d,p) level of theory.[35]

A comparison of the theoretical IR spectra of the low-energy conformers of PG···$(H_2O)_1$ with the experimental IR spectrum of the complex provided in Figure 4 demonstrates that the theoretical IR spectra of the two isoenergetic conformers $C7_D$-$C7_L$-W(I_{NHBn})-4-g^+-*t* and $C7_D$-$C7_L$-W(I_{NHBn})-5-g^+-*c* presented in Figure 4b and c, respectively, are the best matches with the experimental IR spectrum exhibited in Figure 4a. A comparison with the theoretical IR spectra of further higher energy conformers of PG···$(H_2O)_1$ calculated at the M06-2X/6-311++G(d,p) level, is provided in Figure S3. It is clear from the comparison that the global minimum conformer PG-$C7_D$-$C7_L$-W(B_{CO})-1-g^+-*t* obtained from the M06-2X/6-311++G(d,p) level calculation is not the observed structure (Figure 4d), rather the conformer $C7_D$-$C7_L$-W(I_{NHBn})-4-g^+-*t* or $C7_D$-$C7_L$-W(I_{NHBn})-5-g^+-*c* higher in energy by ~ 3.5 kJ/mol is the observed one in the experiment (Figure 4b-c). Obviously, the bridge conformer $C7_D$-$C7_L$-W(B_{CO})-1-g^+-*t* with both the hydrogens of the H_2O molecule hydrogen bonded with the two C=O groups cannot be the observed structure as the experimental IR spectrum shows a free O-H stretching band at 3709 cm^{-1}. Hence, the structure of the single conformer of PG···$(H_2O)_1$ observed in the experiment is the one with the H_2O molecule inserted into the C7 hydrogen bond between the C=O group of Pro and NH group of NHBn of PG, while the other C7 hydrogen bond between the Gly N-H and Boc C=O group remains intact.

The reason behind the observed structure not being the global minimum could be due to the limitation of the M06-2X functional in predicting accurately the relative stability of the monohydrated conformers of PG as the energy difference (ca. 3.5 kJ/mol) between the conformers 1 and 4 is within the computational error. A similar type of assignment of the experimental IR spectrum by the theoretical IR spectrum of a conformer higher in energy than the global minimum was reported recently for N-Acetyl-phenylalanine-amide NAPA$\cdots(H_2O)_1$ and Aspartame$\cdots(H_2O)_2$ complexes.[41, 56] Interestingly, MP2/6-311++G(d,p)//M06-2X/6-311++G(d,p) single-point energy calculations of the low-energy conformers of PG$\cdots(H_2O)_1$ show that the insertion structure $C7_D$-$C7_L$-W(I_{NHBn})-4-g^+-t is indeed the global minimum (Figure 4b). A comparison of the energetics of a few low-energy conformers of PG$\cdots(H_2O)_1$ calculated at the MP2/6-311++G(d,p)//M06-2X/6-311++G(d,p) single-point at 0 K and M06-2X/6-311++G(d,p) levels at both 0 K and 300 K is provided in Table S1. It can be further noticed from Table S1 as well as Figure 4 that $C7_D$-$C7_L$-W($I_{NHB/n}$)-4-g^+-t is more stable than its *cis* counterpart $C7_D$-$C7_L$-W(I_{NHBn})-5-g^+-c and the bridge conformer $C7_D$-$C7_L$-W(B_{CO})-1-g^+-t by 3.92 and 7.56 kJ/mol, respectively, at the MP2 single point level of calculation. Hence, the structure $C7_D$-$C7_L$-W(I_{NHBn})-4-g^+-t, which is assigned as the observed conformer of PG$\cdots(H_2O)_1$, is provided with the observed IR spectrum in Figure 4.

Furthermore, DFT calculations performed at the B3LYP-D3/def2-TZVPP level also predict the insertion structure $C7_D$-$C7_L$-W(I_{NHBn})-5-g^+-c as the most stable conformer, while both $C7_D$-$C7_L$-W(I_{NHBn})-4-g^+-t and $C7_D$-$C7_L$-W(B_{CO})-1-g^+-t are higher in energy only by ~ 0.5 kJ/mol compared to the global minimum (Figure S4 and Table S1). The energy landscape and optimized structures of a few low-energy conformers of PG$\cdots(H_2O)_1$ obtained from the B3LYP-D3/def2-TZVPP level calculations are provided in Figures S4 and S5, respectively. It is intriguing to note that the assigned conformer $C7_D$-$C7_L$-W(I_{NHBn})-4-g^+-t is found to be the most stable conformer also at the MP2/def2-TZVPP//B3LYP-D3/def2-TZVPP single point

level of calculation (Table S1). A comparison of the theoretical IR spectra of the low-energy conformers calculated at the B3LYP-D3/def2-TZVPP level with the experimental IR spectrum of the complex is depicted in Figure S6. Undoubtedly, the theoretical IR spectrum of only the assigned insertion conformer, i.e., $C7_D$-$C7_L$-W(I_{NHBn})-4-g^+-t or $C7_D$-$C7_L$-W(I_{NHBn})-5-g^+-c has a reasonable matching with the experimental IR spectrum. However, the agreement between the experimental IR spectrum of PG$\cdots(H_2O)_1$ and the theoretical IR spectrum of the assigned structure is much better at the M06-2X/6-311++G(d,p) level (Figure 4) than that at the B3LYP-D3/def2-TZVPP level. It seems that the assigned structure obtained from the M06-2X level is close to the observed one, although the energetics of the conformers provided by this level are not satisfactory. The variations of relative energies between one level of theory to another illustrate that the conformational landscape of PG$\cdots(H_2O)_1$ is relatively complex, and the relative depth of the minima is quite sensitive to alterations of the model used to describe them. This reinforces using the observed spectrum as the most robust criterion to evaluate the observed conformation and structure.

Finally, the vibrational bands in the experimental IR spectrum of PG$\cdots(H_2O)_1$ exhibited in Figure 4a are assigned by comparing those with the theoretical IR spectrum of the assigned conformer at the M06-2X/6-311++G(d,p) level presented in Figure 4b. The observed IR band at 3709 cm^{-1} arises due to the antisymmetric stretching frequency of the free dangling O-H group of H_2O. The antisymmetric and symmetric O-H stretching frequencies of free H_2O from gas-phase IR spectroscopy were reported at 3756 and 3658 cm^{-1}, respectively.[35] A small amount of red-shift of 47 cm^{-1} in the stretching frequency of the dangling O-H of H_2O in PG$\cdots(H_2O)_1$ is due to the formation of a strong bridging hydrogen bond by H_2O with the N-H and C=O groups of the backbone. Biswal *et al*. observed the stretching frequency of the free dangling O-H group of H_2O in the monohydrated complex of N-Acetyl-phenylalanine-amide (NAPA) at 3721 cm^{-1}.[41]

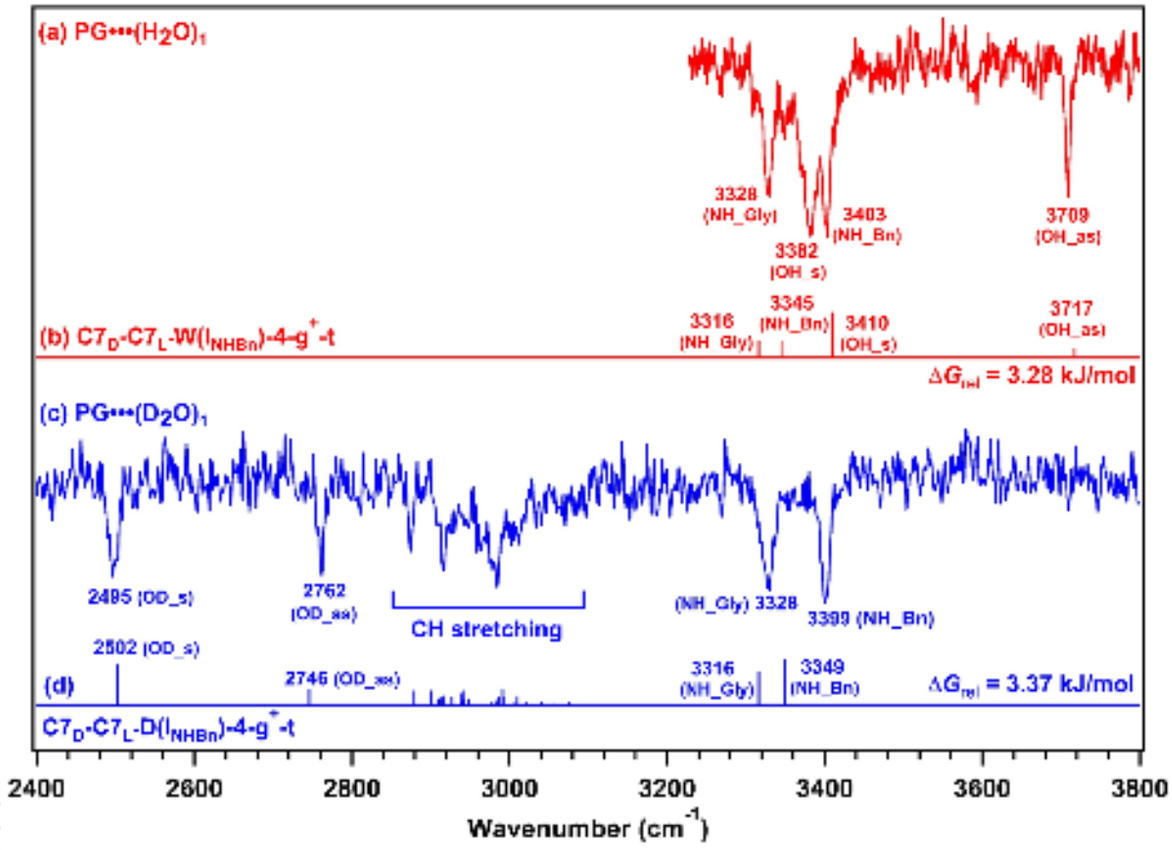

Figure 5. A comparison between the IR spectra of (a) PG···$(H_2O)_1$ and (c) PG···$(D_2O)_1$ measured by RIDIR spectroscopy. (b and d) Theoretical scaled IR stick spectra of the assigned conformers of the PG···$(H_2O)_1$ and PG···$(D_2O)_1$ complexes, respectively, calculated at the M06-2X/6-311++G(d,p) level of theory. ΔG_{rel} values of the three complexes are provided with the stick diagrams. Intensity of the C-H stretching vibrations in the 2850-3100 cm^{-1} region of the theoretical scaled IR stick spectra presented in Figure 5d is multiplied by 3.

The 3328 cm^{-1} band in the IR spectrum provided in Figure 4a is assigned to the N-H stretching frequency of the Gly residue, which is C7 hydrogen-bonded with the Boc C=O group. On the other hand, the assignment of the two close-lying bands at 3382 and 3403 cm^{-1} is not straightforward from the calculations due to a strong coupling between these two frequencies. However, we have assigned the band at 3382 cm^{-1} to the symmetric O-H stretching vibration of H_2O hydrogen-bonded with the Pro C=O group and the 3403 cm^{-1} band to the N-H stretching vibration of the NHBn group hydrogen-bonded with H_2O by identifying the difference in the amplitude of the vibration of these two modes at a particular frequency.

To further confirm the assignments of the IR bands of the observed single conformer of PG···$(H_2O)_1$, mass-selected IR spectrum of 1:1 complexes of PG with D_2O has been measured using RIDIR spectroscopy. The time of flight mass spectrum of PG with D_2O recorded at 35330 cm^{-1} has been provided in Figure S7. Expectedly, the electronic spectra of PG···$(D_2O)_1$ measured, using 2c-R2PI spectroscopy, is similar to that of PG···$(H_2O)_1$, and those two spectra are presented together in Figure S8. Mass-selected IR spectrum of PG···$(D_2O)_1$ measured by probing its electronic band origin is depicted in Figure 5c. The experimental IR spectrum of PG···$(H_2O)_1$ and the theoretical IR spectrum of the assigned structure are reproduced in Figure 5a and b, respectively, to have a comparison with the IR spectrum of the deuterated complex. Theoretical scaled IR spectrum of the same assigned conformer of PG···$(H_2O)_1$ by replacing H_2O with D_2O calculated at the M06-2X/6-311++G(d,p) level is shown in Figure 5d. A scaling factor of 0.951, which has been used to scale the harmonic O-D stretching frequency of D_2O at the M06-2X/6-311++G(d,p) level, is derived from the gas phase experimental O-D stretching frequencies of D_2O reported in the literature.[35] A comparison of the experimental IR spectra of PG···$(D_2O)_1$ with the theoretical IR spectra of their few low-energy conformers calculated at the M06-2X/6-311++G(d,p) level are also provided in Figures S9.

A comparison between the experimental IR spectra of PG···$(H_2O)_1$ and PG···$(D_2O)_1$ presented in Figure 5 reveals unambiguously and irrespective of comparison with calculations that the IR band at 3382 cm^{-1} in PG···$(H_2O)_1$ is due to the hydrogen-bonded O-H group of H_2O as this band is moved to 2495 cm^{-1} position in the PG···$(D_2O)_1$ spectrum. In contrast, the 3328 and 3403 cm^{-1} bands assigned to the hydrogen-bonded Gly N-H and NHBn N-H groups, respectively, remain almost intact in the deuterated complexes of PG. The free O-H band of H_2O is also missing in the PG···$(D_2O)_1$ spectrum, while the free O-D stretching frequency is observed at 2762 cm^{-1}. The bands observed in the 2800-3100 cm^{-1} region in the IR spectrum of

PG…$(D_2O)_1$ are due to C-H stretching vibrations. The calculated harmonic C-H stretching vibrations are scaled using the same scaling factor of 0.943 that has been used to scale the harmonic N-H frequency at the M06-2X/6-311++G(d,p) level. Theoretical scaled C-H stretching vibrations of very weak intensity in PG…$(D_2O)_1$ are exhibited in the IR stick spectra shown in Figure 5d. A clear observation of only two IR bands due to the O-H stretching vibrations also confirms that there is no influence of fragmentation of higher order water clusters of PG into the PG···$(H_2O)_1$ mass channel probed in the experiment. Similar IR spectra were also obtained by probing multiple bands in the electronic spectrum of PG···$(H_2O)_1$.

It should be noted here that the frequencies of the C7 hydrogen-bonded backbone N-H stretching vibrations of the peptides generally appear in the 3310-3420 cm^{-1} range. In the case of PG···$(H_2O)_1$, the C7 hydrogen-bonded N-H stretching frequencies of Gly and NHBn are observed at 3328 and 3403 cm^{-1}, respectively, while those two corresponding frequencies for PG were reported at 3346 and 3391 cm^{-1}, respectively. The hydrogen-bonded (O-H···O) symmetric O-H stretching frequency (3382 cm^{-1}) of H_2O in PG···$(H_2O)_1$ is red-shifted by 276 cm^{-1} with respect to its free symmetric O-H stretching vibration (3658 cm^{-1}).

D. Analysis of the assigned structure of PG···$(H_2O)_1$

The single H_2O molecule is inserted selectively into one of the C7 hydrogen bonds of the PG monomer, keeping the secondary structure similar to that of the monomer. A few selected geometrical specifications, including the Ramachandran angles and hydrogen bond parameters of the assigned structures of the PG monomer[21], i.e., $C7_D$-$C7_L$-g^+-*c* and $C7_D$-$C7_L$-g^+-*t* as well as PG···$(H_2O)_1$, i.e., $C7_D$-$C7_L$-W(I_{NHBn})-4-g^+-*t* calculated at the M06-2X/6-311++G(d,p) level, are listed in Table 1. Chemical structures of the observed conformer of PG···$(H_2O)_1$ with atom numbering and marking of Ramachandran angles and other relevant dihedral angles are provided in Figure 6, while the same for the PG monomer is already depicted in Figure 1a. The hydrogen bond parameters presented in Table 1 indeed reveal that H_2O breaks the C7 hydrogen

bond between the Pro C=O and NHBn N-H groups, which is relatively weaker than the other C7 hydrogen bond present in PG. NBO analysis of the hydrogen bonds present in the PG monomer and PG···$(H_2O)_1$ provided in Figure S10 also indicates that the C7 hydrogen bond

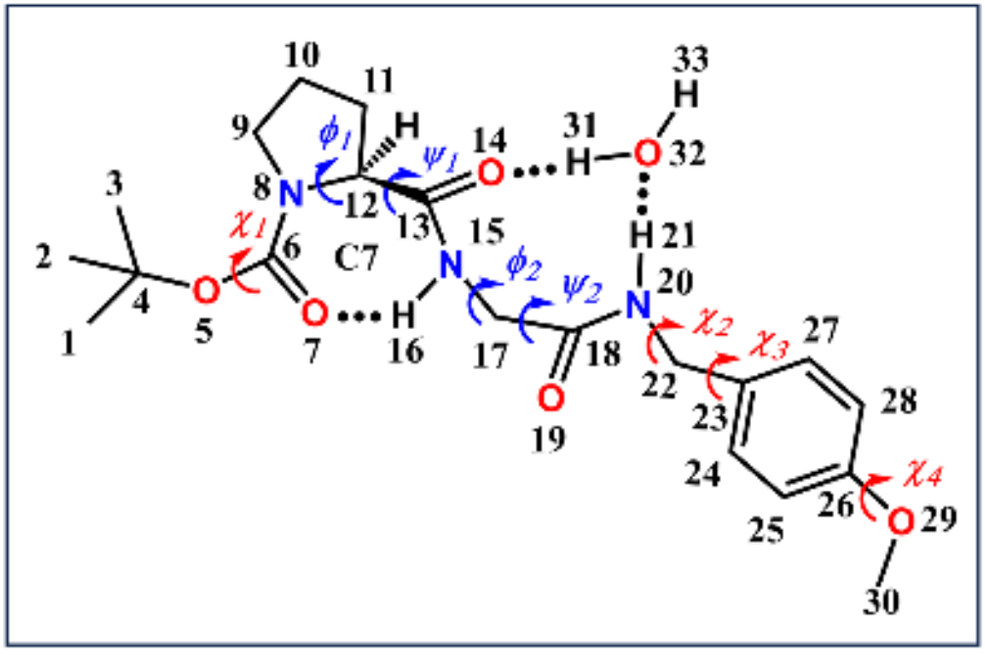

Figure 6. Chemical structure of PG···$(H_2O)_1$ displaying the secondary structure and showing atom numbering as well as important dihedral angles.

involving the NHBn group is weaker than that with the Gly N-H. The NCI plots for the hydrogen bond interactions present in the PG monomer and its monohydrated complex presented in Figure S11 further validate this finding.

A comparison of the backbone Ramachandran angles of the PG monomer and PG···$(H_2O)_1$ exhibited in Table 1 indicates that the secondary structure motif of the PG backbone after complexation with H_2O remains almost similar except the ψ_2 dihedral angle, which is changed from 73.5° to 124.5°. The ψ_2 dihedral angle is related to the NH group of NHBn, which has to accommodate the H_2O molecule to form a bridge hydrogen bond with the Pro C=O group in PG···$(H_2O)_1$. Typical φ, ψ angles for the $C7_D$ (γ_D) structure of peptides are 75° and -65°, respectively, while the those for the $C7_L$ (γ_L) structure are -75° and 65°, respectively. Hence, the single H_2O molecule in PG···$(H_2O)_1$ significantly distorts the peptide backbone, but the

overall secondary structural motif of the PG monomer remains similar. Essentially, the H_2O molecule substantially opens up the C7 hydrogen bond between the NHBn N-H and Pro C=O and fits itself there through double hydrogen bonding interactions.

Table 1. A few selected geometrical parameters, including the Ramachandran angles and hydrogen bond parameters of the two assigned conformers of the PG monomer, i.e., $C7_D$-$C7_L$-g^+-*c*, $C7_D$-$C7_L$-g^+-*t*, and the observed single conformer of PG···$(H_2O)_1$, i.e., $C7_D$-$C7_L$-W(I_{NHBn})-4-g^+-*t* calculated at the M062X/6-311++G(d,p) level of theory. Distances are given in Å unit, while bond angles and dihedral angles are reported in (◦) unit

Geometrical parameters	**PG monomer**		**PG···$(H_2O)_1$**
	PG-$C7_D$-$C7_L$-g^+-*c*	**PG-$C7_D$-$C7_L$-g^+-*t***	**PG-$C7_D$-$C7_L$-W(I_{NHBn})-4-g^+-*t***
ϕ_1 (°)	85.3	85.3	83.3
ψ_1 (°)	-65.0	-70.5	-72.6
ϕ_2 (°)	-80.3	-81.3	-85.3
ψ_2 (°)	73.6	67.2	122.0
χ_1 (°)	173.9	172.8	169.3
χ_2 (°)	83.2	73.5	67.5
χ_3 (°)	99.2	76.2	67.3
χ_4 (°)	-1.6	-173.3	-173.4
$d_{N_{[15]}-H_{[16]}\cdots O_{[7]}}$	1.96	1.97	1.94
$\angle N_{[15]}-H_{[16]}\cdots O_{[7]}$	148.0	146.1	147.8
$d_{N_{[20]}-H_{[21]}\cdots O_{[14]}}$	2.03	2.04	3.30
$\angle N_{[20]}-H_{[21]}\cdots O_{[14]}$	144.0	145.0	105.8
$d_{O_{[32]}-H_{[31]}\cdots O_{[14]}}$	-	-	1.78
$\angle O_{[32]}-H_{[31]}\cdots O_{[14]}$	-	-	167.7
$d_{N_{[20]}-H_{[21]}\cdots O_{[32]}}$	-	-	1.92
$\angle N_{[20]}-H_{[21]}\cdots O_{[32]}$	-	-	157.4

Mons and co-workers described the process of microhydration of peptides during supersonic cooling into three categories.[41] The first one is about hydration without substantial changes in the structures of the peptides, while the second one could be hydration-induced considerable distortion of the peptide backbone without modifying the overall secondary structure. The third category is an alteration of the peptide secondary structure through microhydration. The monohydrate of PG studied here falls under the second category. In the case of the capped phenylalanine model peptide, i.e., CH_3CO-Phe-NH_2, Biswal *et al*. observed that a single H_2O molecule could modify the secondary structure of the peptide from a β-strand to a γ-turn in the gas phase.[41] Gerhards and co-workers observed that the addition of a single H_2O molecule to a model tripeptide Ac-Val-Tyr(Me)-NHMe in the gas phase conserves its β-sheet related secondary structure without any significant changes in the backbone.[44] They further demonstrated from the gas phase spectroscopic study of a monohydrated cyclic tetrapeptide, i.e., cyclo[L-Tyr(Me)-D-Pro]$_2$···$(H_2O)_1$, that the H_2O molecule in one of the isomers of the complex is inserted into an N-H···O=C intramolecular hydrogen bond.[46] Schmidt and coworkers reported that isolated tripeptide model Z-Aib-Pro-NHMe and its microsolvated complex with one CH_3OH molecule exhibited a γ-turn structure while complexation with two CH_3OH switched the γ-turn structure of the peptide to a β-turn, which is the preferred structure in the condensed phase.[45] A comparison of these limited gas phase studies on the microsolvation of the peptides with the monohydrated PG peptide studied here indicates that the second or third H_2O molecule complexed with the PG may prefer the β-turn structure of the peptide that is favorable in the solution phase.

IV. CONCLUSIONS

Microhydration of a capped Pro-Gly dipeptide (PG) or a tripeptide model with a single H_2O molecule has been investigated in the gas phase employing mass-selected R2PI and IR-UV

double resonance spectroscopy combined with detailed quantum chemistry calculations. Observation of a single conformer of the PG···$(H_2O)_1$ complex in the gas phase experiment has been confirmed from IR-UV hole-burning spectroscopy. A comparison of the experimental IR spectrum of the complex with the theoretical IR spectra of several probable low-energy conformers of PG···$(H_2O)_1$ confirms that the observed structure is the one with the H_2O molecule inserted into the relatively weaker C7 hydrogen bond between the C=O group of Pro and NH group of NHBn of PG, while the other stronger C7 hydrogen bond between the Gly N-H and Boc C=O group of the peptide remains intact. The assignment of the observed IR spectrum of the PG···$(H_2O)_1$ complex was further confirmed by measuring the IR spectrum of PG···$(D_2O)_1$ in the gas phase. The observed structure of the PG···$(H_2O)_1$ complex indicates that the single H_2O molecule induces a considerable distortion of the peptide backbone without modifying its overall secondary structure with double γ-turns. In the future, it will be intriguing to explore the microhydration of PG in the gas phase with a few more H_2O molecules to observe whether the γ-turn structure of PG can switch to its favorable condensed phase structure with a β-turn.

SUPPLEMENTARY MATERIAL

See the supplementary material for the IR-UV hole-burning spectra by probing all the IR bands of PG···$(H_2O)_1$, optimized structures of the complex up to ΔG_{rel} = 10 kJ/mol at the M06-2X/6-311++G(d,p) and B3LYP-D3/def2-TZVPP levels of theory, energy landscape of the optimized structures of the complex up to ΔG_{rel} = 10 kJ/mol at the B3LYP-D3/def2-TZVPP level of theory, comparison of the energetics of the structures of the complex at the single point MP2 levels with the DFT levels, comparison of the RIDIR spectrum of the complex with the theoretical IR spectra of probable low-energy conformers at the M06-2X/6-311++G(d,p) and B3LYP-D3/def2-TZVPP levels, TOF mass spectra and electronic spectra of PG with H_2O and

D_2O using 2c-R2PI spectroscopy, NBO and NCI analyses of the hydrogen bonding interactions in PG and PG···$(H_2O)_1$.

ACKNOWLEDGMENTS

The authors gratefully acknowledge the Science and Engineering Research Board (SERB), India (Grant No. CRG/2020/002696) for the partial financial support to carry out the present research. This work is also supported by the France 2030 (PhOM-Graduate School Physique) program, with the reference ANR-11-IDEX-0003. The computational support and resources provided by the 'PARAM Brahma Facility' under the National Supercomputing Mission, Government of India at IISER, Pune, are also acknowledged. SM thanks IISER Pune for his research fellowship. The authors also thank Dr. Satish Kumar for synthesizing the Pro-Gly peptide.

AUTHOR DECLARATIONS

Conflict of Interest

The authors have no conflict to disclose.

Author Contributions

Sourav Mandal: Investigation (equal); Methodology–Theoretical (lead); Formal analysis (equal); Writing–review & edit (equal); validation (equal); **Arsene Kossov:** Investigation (equal); Formal analysis (equal); Methodology–Experimental (lead); Writing–review & edit (equal); validation (equal); **Pierre Carcabal:** Conceptualization (lead); Funding acquisition (lead); Resources (lead); Investigation (lead); Formal analysis (equal); Methodology–Experimental (lead), Writing– review & editing (equal); validation (equal); **Aloke Das:** Conceptualization (lead); Funding acquisition (lead); Resources (lead); Investigation (lead); Formal analysis (equal); Methodology–Experimental (supporting), Theoretical (lead); Visualization (equal); Writing original draft (lead); Writing– review & editing (lead); validation (equal).

DATA AVAILABILITY

The data that support the findings of this study are available from the corresponding author upon reasonable request.

REFERENCES

[1] B. Anfinsen Christian, "Principles that Govern the Folding of Protein Chains," Science, **181,** 223-230 (1973).

[2] K. A. Dill, "Dominant Forces in Protein Folding," Biochemistry, **29,** 7133-7155 (1990).

[3] C. B. Anfinsen, and H. A. Scheraga, "Experimental and theoretical aspects of protein folding," Adv. Protein Chem., **29,** 205-300 (1975).

[4] L. Pauling, R. B. Corey, and H. R. Branson, "The structure of proteins: Two hydrogen-bonded helical configurations of the polypeptide chain," Proc. Natl. Acad. Sci., **37,** 205-211 (1951).

[5] G. D. Rose, L. M. Glerasch, and J. A. Smith, in *Adv. Protein Chem.*, edited by C. B. Anfinsen, J. T. Edsall, and F. M. Richards (Academic Press, 1985), pp. 1-109.

[6] W. R. Krigbaum, and S. P. Knutton, "Prediction of the Amount of Secondary Structure in a Globular Protein from Its Aminoacid Composition," Proc. Natl. Acad. Sci., **70,** 2809-2813 (1973).

[7] P. Y. Chou, and G. D. Fasman, "Prediction of protein conformation," Biochemistry, **13,** 222-245 (1974).

[8] C. Toniolo, "Intramolecularly hydrogen-bonded peptide conformations," Crit. Rev. Biochem. Mol. Biol., **9,** 1-44 (1980).

[9] R. H. Pain, and B. Robson, "Analysis of the Code Relating Sequence to Secondary Structure in Proteins," Nature, **227,** 62-63 (1970).

[10] J. K. Myers, and C. N. Pace, "Hydrogen bonding stabilizes globular proteins," Biophys. J., **71,** 2033-2039 (1996).

[11] P. N. Lewis, F. A. Momany, and H. A. Scheraga, "Folding of Polypeptide Chains in Proteins: A Proposed Mechanism for Folding," Proc. Natl. Acad. Sci., **68,** 2293 (1971).

[12] J. L. Crawford, W. N. Lipscomb, and C. G. Schellman, "The Reverse Turn as a Polypeptide Conformation in Globular Proteins," Proc. Natl. Acad. Sci., **70,** 538 (1973).

[13] S. K. Brahmachari, and V. S. Ananthanarayanan, "Beta-turns in nascent procollagen are sites of posttranslational enzymatic hydroxylation of proline," Proc. Natl. Acad. Sci., **76,** 5119 (1979).

[14] S. K. Brahmachari, R. S. Rapaka, R. S. Bhatnagar, and V. S. Ananthanarayanan, "Proline-containing β-turns in peptides and proteins. II. Physicochemical studies on tripeptides with the Pro-Gly sequence," Biopolymers, **21,** 1107-1125 (1982).

[15] E. R. Stimson, S. S. Zimmerman, and H. A. Scheraga, "Conformational Studies of Oligopeptides Containing Proline and Glycine," Macromolecules, **10,** 1049-1060 (1977).

[16] N. J. Zondlo, "Non-covalent interactions: Fold globally, bond locally," Nat. Chem. Biol., **6,** 567-568 (2010).

[17] E. Gloaguen, M. Mons, K. Schwing, and M. Gerhards, "Neutral peptides in the gas phase: conformation and aggregation issues," Chem. Rev., **120,** 12490-12562 (2020).

[18] E. Gloaguen, and M. Mons, in *Gas-Phase IR Spectroscopy and Structure of Biological Molecules*, edited by A. M. Rijs, and J. Oomens (Springer International Publishing, Cham, Switzerland, 2015), pp. 225-270.

[19] R. J. Plowright, E. Gloaguen, and M. Mons, "Compact Folding of Isolated Four-Residue Neutral Peptide Chains: H-Bonding Patterns and Entropy Effects," Chemphyschem, **12,** 1889-1899 (2011).

[20] S. Kumar, K. K. Mishra, S. K. Singh, K. Borish, S. Dey, B. Sarkar, and A. Das, "Observation of a weak intra-residue C5 hydrogen-bond in a dipeptide containing Gly-Pro sequence," J. Chem. Phys., **151,** 104309 (2019).

[21] S. Kumar, K. Borish, S. Dey, J. Nagesh, and A. Das, "Sequence dependent folding motifs of the secondary structures of Gly-Pro and Pro-Gly containing oligopeptides," Phys. Chem. Chem. Phys., **24,** 18408-18418 (2022).

[22] M. Gerhards, in *Principles of Mass Spectrometry Applied to Biomolecules*, edited by J. Laskin, and C. Lifshitz (John Wiley & Sons, New Jersey, 2006), pp. 3-61.

[23] M. S. de Vries, and P. Hobza, "Gas-phase spectroscopy of biomolecular building blocks," Annu. Rev. Phys. Chem., **58,** 585-612 (2007).

[24] A. Abo-Riziq, L. Grace, B. Crews, M. P. Callahan, T. van Mourik, and M. S. d. Vries, "Conformational Structure of Tyrosine, Tyrosyl-glycine, and Tyrosyl-glycyl-glycine by Double Resonance Spectroscopy," The Journal of Physical Chemistry A, **115,** 6077-6087 (2011).

[25] P. S. Walsh, K. N. Blodgett, C. McBurney, S. H. Gellman, and T. S. Zwier, "Inherent Conformational Preferences of Ac-Gln-Gln-NHBn: Sidechain Hydrogen Bonding Supports a β-Turn in the Gas Phase," Angew. Chem. Int. Ed., **55,** 14618-14622 (2016).

[26] J. C. Dean, E. G. Buchanan, and T. S. Zwier, "Mixed 14/16 Helices in the Gas Phase: Conformation-Specific Spectroscopy of Z-(Gly)n, n = 1, 3, 5," J. Am. Chem. Soc., **134,** 17186-17201 (2012).

[27] W. Chin, I. Compagnon, J.-P. Dognon, C. Canuel, F. Piuzzi, I. Dimicoli, G. von Helden, G. Meijer, and M. Mons, "Spectroscopic Evidence for Gas-Phase Formation of Successive β-Turns in a Three-Residue Peptide Chain," J. Am. Chem. Soc., **127,** 1388-1389 (2005).

[28] E. Gloaguen, R. Pollet, F. Piuzzi, B. Tardivel, and M. Mons, "Gas phase folding of an $(Ala)_4$ neutral peptide chain: spectroscopic evidence for the formation of a β-hairpin H-bonding pattern," Phys. Chem. Chem. Phys., **11,** 11385-11388 (2009).

[29] W. Chin, M. Mons, J.-P. Dognon, F. Piuzzi, B. Tardivel, and I. Dimicoli, "Competition between local conformational preferences and secondary structures in gas-phase model tripeptides as revealed by laser spectroscopy and theoretical chemistry," Phys. Chem. Chem. Phys., **6,** 2700-2709 (2004).

[30] S. Bakels, M.-P. Gaigeot, and A. M. Rijs, "Gas-Phase Infrared Spectroscopy of Neutral Peptides: Insights from the Far-IR and THz Domain," Chem. Rev., **120,** 3233-3260 (2020).

[31] V. Yatsyna, R. Mallat, T. Gorn, M. Schmitt, R. Feifel, A. M. Rijs, and V. Zhaunerchyk, "Conformational Preferences of Isolated Glycylglycine (Gly-Gly) Investigated with IRMPD-VUV Action Spectroscopy and Advanced Computational Approaches," J. Phys. Chem. A, **123,** 862-872 (2019).

[32] A. M. Rijs, and J. Oomens, in *Gas-Phase IR Spectroscopy and Structure of Biological Molecules*, edited by A. M. Rijs, and J. Oomens (Springer International Publishing, Cham, Switzerland, 2015), pp. 1-42.

[33] T. S. Zwier, "The spectroscopy of solvation in hydrogen-bonded aromatic clusters," Annu. Rev. Phys. Chem., **47,** 205-241 (1996).

[34] R. N. Pribble, and T. S. Zwier, "Size-Specific Infrared Spectra of Benzene-(H_2O)n Clusters (n = 1 through 7): Evidence for Noncyclic (H2O)n Structures," Science, **265,** 75-79 (1994).

[35] T. Watanabe, T. Ebata, S. Tanabe, and N. Mikami, "Size-selected vibrational spectra of phenol-(H_2O)n (n=1-4) clusters observed by IR--UV double resonance and stimulated Raman-UV double resonance spectroscopies," J. Chem. Phys., **105,** 408-419 (1996).

[36] T. S. Zwier, "Laser Spectroscopy of Jet-Cooled Biomolecules and Their Water-Containing Clusters: Water Bridges and Molecular Conformation," J. Phys. Chem. A, **105,** 8827-8839 (2001).

[37] P. Butz, R. T. Kroemer, N. A. Macleod, and J. P. Simons, "Hydration of neurotransmitters: a spectroscopic and computational study of ephedrine and its diastereoisomer pseudoephedrine," Phys. Chem. Chem. Phys., **4,** 3566-3574 (2002).

[38] M. N. Blom, I. Compagnon, N. C. Polfer, G. von Helden, G. Meijer, S. Suhai, B. Paizs, and J. Oomens, "Stepwise solvation of an amino acid: The appearance of zwitterionic structures," J. Phys. Chem. A, **111,** 7309-7316 (2007).

[39] L. C. Snoek, R. T. Kroemer, and J. P. Simons, "A spectroscopic and computational exploration of tryptophan-water cluster structures in the gas phase," Phys. Chem. Chem. Phys., **4,** 2130-2139 (2002).

[40] H. Fricke, K. Schwing, A. Gerlach, C. Unterberg, and M. Gerhards, "Investigations of the water clusters of the protected amino acid Ac-Phe-OMe by applying IR/UV double resonance spectroscopy: microsolvation of the backbone," Phys. Chem. Chem. Phys., **12,** 3511-3521 (2010).

[41] H. S. Biswal, Y. Loquais, B. Tardivel, E. Gloaguen, and M. Mons, "Isolated Monohydrates of a Model Peptide Chain: Effect of a First Water Molecule on the Secondary Structure of a Capped Phenylalanine," J. Am. Chem. Soc., **133,** 3931-3942 (2011).

[42] P. Carcabal, R. A. Jockusch, I. Hunig, L. C. Snoek, R. T. Kroemer, B. G. Davis, D. P. Gamblin, I. Compagnon, J. Oomens, and J. P. Simons, "Hydrogen bonding and cooperativity in isolated and hydrated sugars: mannose, galactose, glucose, and lactose," J. Am. Chem. Soc., **127,** 11414-11425 (2005).

[43] A. Camiruaga, G. Goldsztejn, and P. Çarçabal, "Isotopic dependence of intramolecular and intermolecular vibrational couplings in cooperative hydrogen bond networks: singly hydrated phenyl-α-d-mannopyranoside as a case study," Phys. Chem. Chem. Phys., **25,** 12331-12341 (2023).

[44] H. Fricke, A. Gerlach, C. Unterberg, P. Rzepecki, T. Schrader, and M. Gerhards, "Structure of the tripeptide model Ac-Val-Tyr(Me)-NHMe and its cluster with water investigated by IR/UV double resonance spectroscopy," Phys. Chem. Chem. Phys., **6,** 4636-4641 (2004).

[45] H. Zhu, M. Blom, I. Compagnon, A. M. Rijs, S. Roy, G. von Helden, and B. Schmidt, "Conformations and vibrational spectra of a model tripeptide: change of secondary structure upon micro-solvation," Phys. Chem. Chem. Phys., **12,** 3415-3425 (2010).

[46] K. Schwing, C. Reyheller, A. Schaly, S. Kubik, and M. Gerhards, "Structural Analysis of an Isolated Cyclic Tetrapeptide and its Monohydrate by Combined IR/UV Spectroscopy," Chemphyschem, **12,** 1981-1988 (2011).

[47] K. Y. Hung, P. W. R. Harris, and M. A. Brimble, "Use of 'Click Chemistry' for the Synthesis of Tetrazole-Containing Analogues of the Neuroprotective Agent Glycyl-L-prolyl-L-glutamic Acid," Synlett, 1233-1236 (2009).

[48] E. J. Cocinero, and P. Çarçabal, "Carbohydrates," Gas-Phase Ir Spectroscopy and Structure of Biological Molecules, **364,** 299-333 (2015).

[49] T. Lu, Molclus program, Version 1.12, 2023, http://www.keinsci.com/research/molclus.html.

[50] M. J. Frisch, G. W. Trucks, H. B. Schlegel, G. E. Scuseria, M. A. Robb, J. R. Cheeseman, G. Scalmani, V. Barone, G. A. Petersson, H. Nakatsuji, X. Li, M. Caricato, A. V. Marenich, J. Bloino, B. G. Janesko, R. Gomperts, B. Mennucci, H. P. Hratchian, J. V. Ortiz, A. F. Izmaylov, J. L. Sonnenberg, Williams, F. Ding, F. Lipparini, F. Egidi, J. Goings, B. Peng, A. Petrone, T. Henderson, D. Ranasinghe, V. G. Zakrzewski, J. Gao, N. Rega, G. Zheng, W. Liang, M. Hada, M. Ehara, K. Toyota, R. Fukuda, J. Hasegawa, M. Ishida, T. Nakajima, Y. Honda, O. Kitao, H. Nakai, T. Vreven, K. Throssell, J. A. Montgomery Jr., J. E. Peralta, F. Ogliaro, M. J. Bearpark, J. J. Heyd, E. N. Brothers, K. N. Kudin, V. N. Staroverov, T. A. Keith, R. Kobayashi, J. Normand, K. Raghavachari, A. P. Rendell, J. C. Burant, S. S. Iyengar, J. Tomasi, M. Cossi, J. M. Millam, M. Klene, C. Adamo, R. Cammi, J. W. Ochterski, R. L. Martin, K. Morokuma, O. Farkas, J. B. Foresman, and D. J. Fox, Gaussian 09, Revision D.01, Gaussian, Inc., Wallingford, CT, 2009.

[51] S. F. Boys, and F. Bernardi, "The calculation of small molecular interactions by the differences of separate total energies. Some procedures with reduced errors," Mol. Phys., **19,** 553-566 (1970).

[52] E. D. Glendening, C. R. Landis, and F. Weinhold, "NBO 6.0: Natural bond orbital analysis program," J. Comput. Chem., **34,** 1429-1437 (2013).

[53] F. Weinhold, and C. R. Landis, *Valency and Bonding: A Natural Bond Orbital Donor-Acceptor Perspective* (Cambridge University Press, Cambridge, UK, 2005),

[54] J. Contreras-García, E. R. Johnson, S. Keinan, R. Chaudret, J.-P. Piquemal, D. N. Beratan, and W. Yang, "NCIPLOT: A Program for Plotting Noncovalent Interaction Regions," J. Chem. Theory Comput., **7,** 625-632 (2011).

[55] T. Lu, and F. W. Chen, "Multiwfn: A multifunctional wavefunction analyzer," J. Comput. Chem., **33,** 580-592 (2012).

[56] P. Pinillos, A. Camiruaga, F. Torres-Hernández, P. Çarçabal, I. Usabiaga, J. A. Fernández, and R. Martínez, "Aspartame and Its Microhydrated Aggregates Revealed by Laser

Spectroscopy: Water-Sweetener Interactions in the Gas Phase," J. Phys. Chem. A, **128,** 6714-6721 (2024).